mathematics

MDPI

Article

Shear Waves in an Elastic Plate with a Hole Resting on a Rough Base

Anatoly Nikolaevich Filippov

Department of Higher Mathematics, Gubkin University, Leninsky Prospect 65, Bld. 1, 119991 Moscow, Russia; filippov.a@gubkin.ru; Tel.: +7-(499)-507-8675

Abstract: The article is devoted to the analytical and numerical study of the pattern of propagation and attenuation, due to Coulomb friction, of shear waves in an infinite elastic thin plate with a circular orifice of radius r_0 lying on a rough base. Considering the friction forces and their influence on the sample of wave propagation in extended rods or thin plates is important for calculating the stress–strain state in them and the size of the area of motion. An exact analytical solution of a nonlinear boundary value problem for tangential stresses and velocities is obtained in quadratures by the Laplace transform, with respect to time. It turned out that the complete exhaustion of the wave front of a strong rupture occurs at a finite distance $r*$ from the center of the orifice, and an elementary formula is given for this distance (the case of tangential shock stresses suddenly applied to the orifice boundary is considered). For various ratios of the magnitude of the limiting friction force to the amplitude of the applied load, the stopping (trailing) wave fronts are calculated. After passing them, a state of static equilibrium between the elastic and friction forces with a nonlinear distribution of residual stresses is established in the region $r_0 \leq r \leq r*$. For the first time, a precise analytical solution was obtained for the boundary value problem of the propagation of elastic shear waves in an infinite isotropic space with a cylindrical cavity, when a tangential shock load is set on its surface.

Keywords: shear wave; dry friction; elastic plate with orifice; non-linear partial equations; residual stresses; trailing wave front

MSC: 74H05; 44A10; 35L50; 33E20

Citation: Filippov, A.N. Shear Waves in an Elastic Plate with a Hole Resting on a Rough Base. *Mathematics* **2024**, *12*, 165. https://doi.org/10.3390/math12010165

Academic Editor: Hovik Matevossian

Received: 8 November 2023
Revised: 21 December 2023
Accepted: 3 January 2024
Published: 4 January 2024

1. Introduction

In engineering practice, important tasks often arise for bodies whose transverse dimensions are significantly smaller than longitudinal ones (rods, plates, etc.). Wave motion in such objects drastically depends on the dynamic contact interaction of these bodies with the environment. Such tasks include, for example, the calculation of pile driving, the interaction of an underground pipeline with the ground, various friction devices—for example, clutch discs in cars. The determining role in such devices is played by the friction force that occurs on the contact surfaces both during wave motion and at its completion. The pattern of propagation and attenuation of elastic waves significantly depends on the magnitude of the friction force that attracts the close attention of researchers. For example, dynamics of elastic rods considering the dry friction law interaction with surrounding media is studied in [1]. The monograph [2] provides a detailed review of papers published before 1997 and devoted to interaction of an elastic rod and a rigid medium with a constant dry friction force acting on the contact surface in the presence of relative motion. The mentioned monograph presents exact analytical solutions to the problems of statics and dynamics of elastic and elastoplastic bodies with dry friction, as well as modeling of impact on a pipeline located in an elastic medium. A non-linear mathematical model of dynamic processes that appear under the stuck drill string release, using pulse installations with

consideration of the internal and external friction, is developed in [3]. Authors of [3] found that the dry friction arising on the interaction surfaces of the drill string and the drill mud has a significant influence on the longitudinal wave propagation in the drill string. Elastic wave propagation in a cylindrical body in the presence of Coulomb friction on the contact surface with another nondeformable body and induced by the propagating wave parameters is considered in [4]. It is shown that the accumulation of elastic energy in sliding plates on both sides of the fault can cause fluctuations in the sliding velocity, even with constant friction [5]. The authors of [6] study the problem of longitudinal wave propagation in an elastic rod attached to a locally damaged foundation through a thin elastic layer. In [7], an exact solution to the problem of the wave motion of a semi-infinite rod interacting with a surrounding elastic medium according to the dry friction law under the action of an exponentially dropping dynamic load on the butt of the rod and under a finite mass impact by a rigid body is obtained. It should be noted that there are no articles in the literature known to us where dynamic problems for plates on a rough base are considered.

In this paper, an exact analytical solution is given in quadratures to the boundary value problem of the propagation of elastic shear waves in a thin plate having a circular orifice. The plate is pressed against a rough base by uniform pressure and suddenly applied constant loading acts at the boundary of the orifice. Due to the braking action of friction forces, the shear wave gradually degenerates at a finite distance from the orifice. The radius and the moment of time of complete exhaustion of the elastic wave front are determined. For various values of the ratio of the specific friction force to the load magnitude, the trailing (stopping) fronts of the elastic wave are found. After the passage of these fronts, a state of statical equilibrium occurs between the elastic and dry friction forces in the annular region of the plate adjacent to the orifice. Along the way, formulas for the originals of some Laplace transformants are obtained, which are not found in the known literature.

2. Setting of the Boundary Value Problem

Consider an infinite elastic homogeneous plate of constant thickness h, with a circular cutout of radius r_0, lying on a hard, rough base and interacting with it according to Coulomb's dry friction law (Figure 1). In the case where there is a slip between the plate and the base, a friction force will act on an arbitrary part of the contact surface of area S, the magnitude of which is equal in modulus fNS, where N—pressure on the plate and f—the coefficient of friction between the materials of the plate and the base. In the absence of slippage, the friction force takes on some values, generally speaking, not the same at different points of the plate, but not exceeding the absolute value of the limit.

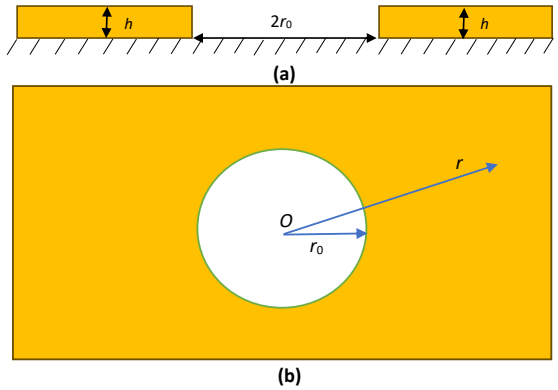

Figure 1. Plate with a circular orifice on the rough base: (**a**) Plate cross section. (**b**) View from above.

In the problem under consideration, as well as in [1–6], we will consider the limiting friction force to be constant. In the case when h is small compared to the characteristic propagation length of the elastic pulse, the stress change over the thickness of the plate can be neglected and the friction force can be considered as a volumetric one with density $\eta = fN/h$.

Let us choose the beginning of the polar coordinate system in the center of the cutout (Figure 1). Prior to the application of the load, we consider the plate to be at rest, unstressed and undeformed. At time $t = 0$, tangential forces are applied instantly to the boundary of the orifice $r = r_0$ so that the magnitude of these forces does not depend on the polar angle and is maintained constant in time. Then, due to the symmetry of the problem, the tangential stresses $\tau(r,t)$ and the transversal velocity $v(r,t)$ satisfy the following system of partial differential equations:

$$\begin{array}{l} \frac{\partial \tau}{\partial r} + 2\frac{\tau}{r} = \frac{\partial v}{\partial t} + \kappa q, \\ \frac{\partial \tau}{\partial t} = \frac{\partial v}{\partial r} - \frac{v}{r}. \end{array} \quad (1)$$

Dimensionless variables and quantities are used here: the stress is related to the shear modulus μ of the plate material, the velocity is related to the velocity of transverse elastic waves $c_\tau = \sqrt{\mu/\rho}$ (ρ—the plate material density), the radial coordinate r is related to the radius of the hole r_0, time t—by the time the shear wave travels a distance equal to the radius of the hole r_0, and the friction parameter $q = r_0 fN/(h\mu) = r_0\eta/\mu$ is introduced. The value of κ in the case of motion coincides with the sign of velocity, and in the case of rest, takes some values from the interval $(-1;1)$, depending on the radial coordinate of the circular cross section under consideration, and is determined further from the solution of the problem.

We assume that in the presence of motion $v(r,t) > 0$. Then, in (1), it should be put $\kappa = \mathrm{H}(t - r + 1)$, since in the area before of the elastic wave front $t = r - 1$, the friction force is zero (here, $\mathrm{H}(x)$ is the Heaviside function). In the accepted notations, the initial and boundary conditions acquire, respectively, the form:

$$\tau = v = \kappa = 0 \,\text{at}\, t = 0,\ r > 1, \quad (2)$$

$$\tau = -\tau_0 \mathrm{H}(t) \,\text{at}\, r = 1,\ t \geq 0. \quad (3)$$

where τ_0—positive dimensionless constant.

3. Solution of the Boundary Value Problem

3.1. Laplace Transform

The solution of the boundary value problem (1)–(3) is sought using the Laplace time transform method. Applying the transform to the equations of system (1) and boundary condition (3), and also taking into account (2), we obtain a system of two ordinary differential equations with respect to images of stress $T(r,p)$ and velocity $V(r,p)$:

$$\begin{array}{l} \frac{dT}{dr} + 2\frac{T}{r} - q\frac{\mathrm{e}^{-p(r-1)}}{p} = pV, \\ pT = \frac{dV}{dr} - \frac{V}{r}, \end{array} \quad (4)$$

where

$$T(r,p) = \int_0^\infty \tau(r,t)\mathrm{e}^{-pt}dt,\ V(r,p) = \int_0^\infty v(r,t)\mathrm{e}^{-pt}dt, \quad (5)$$

and p is the transform parameter.

The boundary condition (3) in the images takes the form:

$$T(1,p) = -\frac{\tau_0}{p}. \quad (6)$$

3.2. Getting a Solution in Images

From (4), it is easy to obtain second-order ordinary differential equations for transformants $T(r,p)$ and $V(r,p)$:

$$\frac{d^2T}{dr^2} + \frac{1}{r}\frac{dT}{dr} - \left(p^2 + \frac{4}{r^2}\right)T = -q\left(1 + \frac{1}{rp}\right)\mathrm{e}^{-p(r-1)}, \quad (7)$$

$$\frac{d^2V}{dr^2} + \frac{1}{r}\frac{dV}{dr} - \left(p^2 + \frac{1}{r^2}\right)V = q\mathrm{e}^{-p(r-1)}. \tag{8}$$

Let us introduce a new variable y instead of r by the formula: $y = pr$. In this case, Equations (7) and (8) will be rewritten as:

$$\frac{d^2T}{dy^2} + \frac{1}{y}\frac{dT}{dy} - \left(1 + \frac{2^2}{y^2}\right)T = -\frac{q}{p^2}\left(1 + \frac{1}{y}\right)\mathrm{e}^{p-y}, \tag{9}$$

$$\frac{d^2V}{dy^2} + \frac{1}{y}\frac{dV}{dy} - \left(1 + \frac{1}{y^2}\right)V = \frac{q}{p^2}\mathrm{e}^{p-y}. \tag{10}$$

The homogeneous equations corresponding to (9) and (10) are Bessel differential equations, and their general solutions vanishing at infinities, $y \to +\infty$, $r \to +\infty$, are represented [8] as:

$$T_0(y,p) = A \times \mathrm{K}_2(y),\ V_0(y,p) = B \times \mathrm{K}_1(y), \tag{11}$$

where $\mathrm{K_n}(y)$—MacDonald function of order n.

Partial solutions of Equations (9) and (10) have the following form:

$$T_p(y,p) = \frac{q}{3p^2}y\mathrm{e}^{p-y},\ V_p(y,p) = -\frac{q}{3p^2}y\mathrm{e}^{p-y}. \tag{12}$$

Returning to the variable r, taking into account (11) and (12), we arrive at the general solution of Equations (9) and (10), respectively, in the form:

$$T(r,p) = A \times \mathrm{K}_2(pr) + \frac{qr}{3p}\mathrm{e}^{-p(r-1)}, \tag{13}$$

$$V(r,p) = B \times \mathrm{K}_1(pr) - \frac{qr}{3p}\mathrm{e}^{-p(r-1)}. \tag{14}$$

To find the constants A and B in the solutions (13) and (14), we use the boundary condition (6) and the second of Equation (4). As a result, we obtain the following expressions for stress and velocity transformants:

$$T(r,p) = -\left(\tau_0 + \frac{q}{3}\right)\frac{\mathrm{K}_2(pr)}{p\mathrm{K}_2(p)} + \frac{qr}{3p}\mathrm{e}^{-p(r-1)}, \tag{15}$$

$$V(r,p) = \left(\tau_0 + \frac{q}{3}\right)\frac{\mathrm{K}_1(pr)}{p\mathrm{K}_2(p)} - \frac{qr}{3p}\mathrm{e}^{-p(r-1)}. \tag{16}$$

For the transition from $T(r,p)$ and $V(r,p)$ to $\tau(r,t)$ and $v(r,t)$ in Formulas (15) and (16), it is necessary to calculate the originals of the functions of a complex variable p:

$$f_1(p) = \frac{\mathrm{K}_1(pr)}{p\mathrm{K}_2(p)},\ f_2(p) = \frac{\mathrm{K}_2(pr)}{p\mathrm{K}_2(p)}, \tag{17}$$

which, apparently, are not found in the known literature. The originals of the additional terms in Formulas (15) and (16) have the form:

$$\frac{qr}{3p}\mathrm{e}^{-p(r-1)} \leftrightarrow \frac{qr}{3}\mathrm{H}(t-r-1). \tag{18}$$

3.3. Inversion of Laplace's Images

To determine the originals of the images (17), we will perform contour integration. The MacDonald function $\mathrm{K_n}(z)$ ($n \in \mathbb{Z}$) of the complex variable z is analytic on the entire complex plane, with a cut along the negative part of the real axis [8]. Consider the closed contour *ACDEFA* (Figure 2), consisting of arcs *BC* and *FA* of a large circle of radius R

centered at point $p = 0$ of the complex plane p, as well as an arc DE of a small circle of radius ε centered at the same point, a segment AB of a vertical line $p = \gamma + i\infty$ (here $\gamma > 0$) and the shores of the CD and EF cuts. The MacDonald function $K_2(p)$ inside the specified contour, bypassed so that the area it bounds remains on the left, has only two complex-conjugate zeros [8]:

$$z_0 = -x_0 + iy_0, \bar{z}_0 = -x_0 - iy_0. \tag{19}$$

The values of x_0 and y_0 with an accuracy of nine significant digits after the decimal point are equal [9]:

$$x_0 = 1.28137380, \; y_0 = 0.429484965. \tag{20}$$

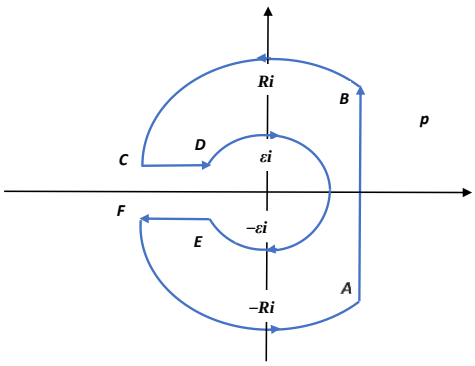

Figure 2. The contour of integration in the complex plane p.

We apply the residue theorem [10] to functions $f_1(p)e^{pt}$ and $f_2(p)e^{pt}$ that are unambiguous and analytic inside a closed contour $ABCDEF$, with the exception of points $p = z_0$ and $p = \bar{z}_0$, in which both functions have simple poles. At the same time, we have:

$$\frac{1}{2\pi i}\int\limits_{ABCDEFA} \frac{K_1(pr)}{pK_2(p)}e^{pt}dp = \sum_{\substack{p=z_0\\ p=\bar{z}_0}} Res\frac{K_1(pr)}{pK_2(p)}e^{pt}, \tag{21}$$

$$\frac{1}{2\pi i}\int\limits_{ABCDEFA} \frac{K_2(pr)}{pK_2(p)}e^{pt}dp = \sum_{\substack{p=z_0\\ p=\bar{z}_0}} Res\frac{K_2(pr)}{pK_2(p)}e^{pt}. \tag{22}$$

First, we transform the integral in (22), dividing it into integrals along smooth contour pieces. Since on the arcs BC and FA we have, respectively:

$$p = Re^{i\varphi}, \; \text{arctg}\frac{R}{\gamma} < \varphi < \pi,$$

$$p = Re^{i\varphi}, \; -\pi < \varphi < -\text{arctg}\frac{R}{\gamma}$$

and $dp = ipd\varphi$; then, tending the radius R to infinity and taking into account the asymptotics of $K_n(z)$ under $|z| \to \infty$ [8]:

$$K_n(z) \simeq \sqrt{\frac{\pi}{2z}}e^{-z},$$

by Jordan's lemma [11] we will have under $t > r - 1$:

$$\begin{gathered}\frac{1}{2\pi i}\lim\limits_{R\to+\infty}\int\limits_{BC} f_2(p)\mathrm{e}^{pt}dp = \frac{1}{2\pi i}\lim\limits_{R\to+\infty}\int\limits_{\arctan\frac{R}{\gamma}}^{\pi}\frac{i\mathrm{K}_2\left(r\mathrm{Re}^{i\varphi}\right)}{\mathrm{K}_2\left(R\mathrm{e}^{i\varphi}\right)}\mathrm{e}^{tR\mathrm{e}^{i\varphi}}d\varphi = \\ \frac{1}{2\pi}\int\limits_{\frac{\pi}{2}}^{\pi}\lim\limits_{R\to+\infty}\left[\sqrt{\frac{\pi}{2rR\mathrm{e}^{i\varphi}}}\mathrm{e}^{-rR\mathrm{e}^{i\varphi}}\sqrt{\frac{2R\mathrm{e}^{i\varphi}}{\pi}}\mathrm{e}^{R\mathrm{e}^{i\varphi}}\mathrm{e}^{tR\mathrm{e}^{i\varphi}}\right]d\varphi = \frac{1}{2\pi\sqrt{r}}\int\limits_{\frac{\pi}{2}}^{\pi}\lim\limits_{R\to+\infty}\mathrm{e}^{(t-r+1)R\mathrm{e}^{i\varphi}}d\varphi = 0,\end{gathered} \tag{23}$$

$$\frac{1}{2\pi i}\lim\limits_{R\to+\infty}\int\limits_{FA} f_2(p)\mathrm{e}^{pt}dp = \frac{1}{2\pi\sqrt{r}}\int\limits_{-\pi}^{-\frac{\pi}{2}}\lim\limits_{R\to+\infty}\mathrm{e}^{(t-r+1)R\mathrm{e}^{i\varphi}}d\varphi = 0. \tag{24}$$

In exactly the same way, we get:

$$\frac{1}{2\pi i}\lim\limits_{R\to+\infty}\int\limits_{BC} f_1(p)\mathrm{e}^{pt}dp = 0,\ \frac{1}{2\pi i}\lim\limits_{R\to+\infty}\int\limits_{FA} f_1(p)\mathrm{e}^{pt}dp = 0 \text{ under } t > r - 1. \tag{25}$$

On the contour DE of a small circle, we have $p = \varepsilon\mathrm{e}^{i\varphi}$, where φ decreases from π to $-\pi$. Tending the radius ε to zero and considering that $\mathrm{K}_1(z) \sim \frac{1}{z}$, $\mathrm{K}_2(z) \sim \frac{2}{z^2}$ under $|z| \to 0$, we have:

$$\begin{gathered}\frac{1}{2\pi i}\lim\limits_{\varepsilon\to0}\int\limits_{DE} f_2(p)\mathrm{e}^{pt}dp = \frac{1}{2\pi i}\lim\limits_{\varepsilon\to0}\int\limits_{\pi}^{-\pi}\frac{i\mathrm{K}_2\left(r\varepsilon\mathrm{e}^{i\varphi}\right)}{\mathrm{K}_2\left(\varepsilon\mathrm{e}^{i\varphi}\right)}\mathrm{e}^{t\varepsilon\mathrm{e}^{i\varphi}}d\varphi = \\ \frac{1}{2\pi}\lim\limits_{\varepsilon\to0}\int\limits_{\pi}^{-\pi}\frac{\mathrm{e}^{t\varepsilon\mathrm{e}^{i\varphi}}}{r^2}d\varphi = \frac{1}{2\pi r^2}\lim\limits_{\varepsilon\to0}\int\limits_{\pi}^{-\pi}d\varphi = -\frac{1}{r^2},\end{gathered} \tag{26}$$

$$\begin{gathered}\frac{1}{2\pi i}\lim\limits_{\varepsilon\to0}\int\limits_{DE} f_1(p)\mathrm{e}^{pt}dp = \frac{1}{2\pi}\lim\limits_{\varepsilon\to0}\int\limits_{\pi}^{-\pi}\frac{\mathrm{K}_1\left(r\varepsilon\mathrm{e}^{i\varphi}\right)}{\mathrm{K}_2\left(\varepsilon\mathrm{e}^{i\varphi}\right)}\mathrm{e}^{t\varepsilon\mathrm{e}^{i\varphi}}d\varphi = \\ \frac{1}{2\pi}\lim\limits_{\varepsilon\to0}\int\limits_{\pi}^{-\pi}\frac{1}{r\varepsilon\mathrm{e}^{i\varphi}}\frac{\varepsilon^2\mathrm{e}^{2i\varphi}}{2}\mathrm{e}^{t\varepsilon\mathrm{e}^{i\varphi}}d\varphi = \frac{1}{4\pi r}\lim\limits_{\varepsilon\to0}\int\limits_{\pi}^{-\pi}\varepsilon\mathrm{e}^{t\varepsilon\mathrm{e}^{i\varphi}}\mathrm{e}^{i\varphi}d\varphi = 0.\end{gathered} \tag{27}$$

Let us now consider integrals along the shores of the cut CD and EF. Noticing that:

$$p = ze^{i\pi},\ \varepsilon < z < R \text{ along } CD;\ p = ze^{-i\pi},\ \varepsilon < z < R \text{ along } EF, \tag{28}$$

and considering the relation $\mathrm{K}_\nu\left(z\mathrm{e}^{\pm\pi i}\right) = e^{\mp\nu\pi i}\mathrm{K}_\nu(z) \mp \pi i\mathrm{I}_\nu(z)$ known in the theory of Bessel functions [8], where $z \in \mathbb{R}^+$, and $\mathrm{I}_\nu(z)$ is the Bessel function of an imaginary argument of order ν, we obtain a series of equalities:

$$\begin{gathered}\mathrm{K}_2\left(z\mathrm{e}^{\pi i}\right) = \mathrm{K}_2(z) - \pi i\mathrm{I}_2(z),\ \mathrm{K}_2\left(z\mathrm{e}^{-\pi i}\right) = \mathrm{K}_2(z) + \pi i\mathrm{I}_2(z), \\ \mathrm{K}_1\left(z\mathrm{e}^{\pi i}\right) = -\mathrm{K}_1(z) - \pi i\mathrm{I}_1(z),\ \mathrm{K}_1\left(z\mathrm{e}^{-\pi i}\right) = -\mathrm{K}_1(z) + \pi i\mathrm{I}_1(z),\ z \in \mathbb{R}^+.\end{gathered} \tag{29}$$

Taking into account (28) and (29), we make the necessary calculations:

$$\begin{gathered}\frac{1}{2\pi i}\lim\limits_{\substack{\varepsilon\to0\\R\to\infty}}\left(\int\limits_{CD} f_2(p)\mathrm{e}^{pt}dp + \int\limits_{EF} f_2(p)\mathrm{e}^{pt}dp\right) = \\ \frac{1}{2\pi i}\lim\limits_{\substack{\varepsilon\to0\\R\to\infty}}\left(\int\limits_{R}^{\varepsilon}\frac{\mathrm{K}_2\left(rze^{i\pi}\right)}{ze^{i\pi}\mathrm{K}_2\left(ze^{i\pi}\right)}\mathrm{e}^{-tz}\mathrm{e}^{i\pi}dz + \int\limits_{\varepsilon}^{R}\frac{\mathrm{K}_2\left(rze^{-i\pi}\right)}{ze^{-i\pi}\mathrm{K}_2\left(ze^{-i\pi}\right)}\mathrm{e}^{-tz}\mathrm{e}^{i\pi}dz\right) = \\ \frac{1}{2\pi i}\left(\int\limits_{\infty}^{0}\frac{\mathrm{K}_2(rz)-\pi i\mathrm{I}_2(rz)}{\mathrm{K}_2(z)-\pi i\mathrm{I}_2(z)}\frac{\mathrm{e}^{-tz}}{z}dz + \int\limits_{0}^{\infty}\frac{\mathrm{K}_2(rz)+\pi i\mathrm{I}_2(rz)}{\mathrm{K}_2(z)+\pi i\mathrm{I}_2(z)}\frac{\mathrm{e}^{-tz}}{z}dz\right) = \\ -\int\limits_{0}^{\infty}\frac{\mathrm{K}_2(rz)\mathrm{I}_2(z)-\mathrm{I}_2(rz)\mathrm{K}_2(z)}{\mathrm{K}_2^2(z)+\pi^2\mathrm{I}_2^2(z)}\frac{\mathrm{e}^{-tz}}{z}dz,\end{gathered} \tag{30}$$

$$\frac{1}{2\pi i}\lim_{\substack{\varepsilon\to 0\\ R\to\infty}}\left(\int\limits_{CD} f_1(p)e^{pt}dp+\int\limits_{EF} f_1(p)e^{pt}dp\right)=\int\limits_0^\infty \frac{K_1(rz)I_2(z)+I_1(rz)K_2(z)}{K_2^2(z)+\pi^2I_2^2(z)}\frac{e^{-tz}}{z}dz. \quad (31)$$

Now let us calculate the sum of residues in (21) and (22). To do this, we need the following formulas linking the modified Bessel functions and their derivatives:

$$zK_\nu^{/}(z)+\nu K_\nu(z)=-zK_{\nu-1}(z). \quad (32)$$

It is known that if $z = z_0$ is a simple zero of the function $\psi(z)$ and $\varphi(z_0)\neq 0$, then we have [10]: $\underset{z=z_0}{Res}\frac{\varphi(z)}{\psi(z)}=\frac{\varphi(z_0)}{\psi'(z_0)}$.

Therefore, given (32) when $\nu = 2$ and $K_2(z_0)=0$, $K_2(\overline{z}_0)=0$, we have:

$$\sum_{\substack{p=z_0\\ p=\overline{z}_0}} Res\frac{K_2(pr)}{pK_2(p)}e^{pt}=\frac{K_2(rz_0)}{z_0K_2^{/}(z_0)}e^{z_0t}+\frac{K_2(r\overline{z}_0)}{\overline{z}_0K_2^{/}(\overline{z}_0)}e^{\overline{z}_0t}=-2\frac{\mathrm{Re}\left[\overline{z}_0K_1(\overline{z}_0)K_2(rz_0)e^{z_0t}\right]}{|z_0|^2|K_1(z_0)|^2}, \quad (33)$$

$$\sum_{\substack{p=z_0\\ p=\overline{z}_0}} Res\frac{K_1(pr)}{pK_2(p)}e^{pt}=-2\frac{\mathrm{Re}\left[\overline{z}_0K_1(\overline{z}_0)K_1(rz_0)e^{z_0t}\right]}{|z_0|^2|K_1(z_0)|^2}. \quad (34)$$

Substituting calculated integrals (23), (24), (26), (27), (30) and (31), and also the relations (33) and (34) in Formulas (21) and (22) and taking into account that

$$\frac{1}{2\pi i}\lim_{R\to+\infty}\int\limits_{AB} f_2(p)e^{pt}dp=\frac{1}{2\pi i}\int\limits_{\gamma-i\infty}^{\gamma+i\infty}\frac{K_2(pr)}{K_2(p)}e^{pt}dp,$$
$$\frac{1}{2\pi i}\lim_{R\to+\infty}\int\limits_{AB} f_1(p)e^{pt}dp=\frac{1}{2\pi i}\int\limits_{\gamma-i\infty}^{\gamma+i\infty}\frac{K_1(pr)}{K_2(p)}e^{pt}dp,$$

we will get new operational relations:

$$\frac{K_1(pr)}{pK_2(p)}\leftrightarrow-\int\limits_0^\infty\frac{K_1(rz)I_2(z)+I_1(rz)K_2(z)}{K_2^2(z)+\pi^2I_2^2(z)}\frac{e^{-tz}}{z}dz-2\frac{\mathrm{Re}\left[\overline{z}_0K_1(\overline{z}_0)K_1(rz_0)e^{z_0t}\right]}{|z_0|^2|K_1(z_0)|^2},\ t>r-1, \quad (35)$$

$$\frac{K_2(pr)}{pK_2(p)}\leftrightarrow\frac{1}{r^2}+\int\limits_0^\infty\frac{K_2(rz)I_2(z)-I_2(rz)K_2(z)}{K_2^2(z)+\pi^2I_2^2(z)}\frac{e^{-tz}}{z}dz-2\frac{\mathrm{Re}\left[\overline{z}_0K_1(\overline{z}_0)K_2(rz_0)e^{z_0t}\right]}{|z_0|^2|K_1(z_0)|^2},\ t>r-1. \quad (36)$$

4. Analysis of the Pattern of Shear Wave Propagation and Discussion

4.1. Determination of True Velocities and Stresses

Since the originals of functions (17) are determined by the relations (35) and (36), then the transition to the true stresses and velocities in (15) and (16) is not difficult. To shorten and make numerical calculations easier, we introduce new ratios by formulas:

$$\sigma=\frac{\tau}{\tau_0},\ w=\frac{v}{\tau_0},\ \alpha=\frac{q}{3\tau_0}. \quad (37)$$

Taking into account (37), the formulas for the stress σ and the velocity w in the region of motion $t > r - 1$, where the velocity is positive, will be written as follows:

$$\sigma(r,t)=\alpha r-\frac{1+\alpha}{r^2}+(1+\alpha)\left(2\frac{\mathrm{Re}\left[\overline{z}_0K_1(\overline{z}_0)K_2(rz_0)e^{z_0t}\right]}{|z_0|^2|K_1(z_0)|^2}-\int\limits_0^\infty\frac{K_2(rz)I_2(z)-I_2(rz)K_2(z)}{K_2^2(z)+\pi^2I_2^2(z)}\frac{e^{-tz}}{z}dz\right), \quad (38)$$

$$w(r,t) = -\alpha r + (1+\alpha)\left(-2\frac{\mathrm{Re}\left[\bar{z}_0 \mathrm{K}_1(\bar{z}_0)\mathrm{K}_1(rz_0)\mathrm{e}^{z_0 t}\right]}{|z_0|^2 |\mathrm{K}_1(z_0)|^2} - \int_0^\infty \frac{\mathrm{K}_1(rz)\mathrm{I}_2(z) + \mathrm{I}_1(rz)\mathrm{K}_2(z)}{\mathrm{K}_2^2(z) + \pi^2 \mathrm{I}_2^2(z)} \frac{\mathrm{e}^{-tz}}{z} dz\right). \quad (39)$$

In this case, the system (1) written with respect to $\sigma(r,t)$ and $w(r,t)$ will take the following form:

$$\frac{\partial \sigma}{\partial r} + 2\frac{\sigma}{r} = \frac{\partial w}{\partial t} + 3\alpha\kappa, \quad (40)$$

$$\frac{\partial \sigma}{\partial t} = \frac{\partial w}{\partial r} - \frac{w}{r}. \quad (41)$$

The solutions presented by Formulas (38) and (39) are valid only in that part of the phase plane (r,t), where $w(r,t) > 0$.

4.2. Determination of the Stopping Front of Circular Sections of the Plate

Suppose that a curve on which the velocity of circular sections $w(r,t)$ turns to zero is found, and its equation is

$$t = \varphi(r), \quad (42)$$

at the same time as

$$w(r, \varphi(r)) = 0. \quad (43)$$

Differentiating (43) by the variable r and denoting the acceleration at the leading wave front as $a_\varphi(r) \equiv \frac{\partial w^+}{\partial t}(r, \varphi(r))$, we find that

$$\frac{\partial w^+}{\partial r}(r, \varphi(r)) = -a_\varphi(r)\varphi'(r). \quad (44)$$

Here, the superscript "+" means that partial derivatives are taken from the side of the domain $t > \varphi(r)$. From Equations (41) and (42), it is easy to obtain the following relations:

$$\frac{\partial \sigma^+}{\partial r}(r, \varphi(r)) = -2\frac{\sigma(r, \varphi(r))}{r} + a_\varphi(r) + 3\alpha\kappa, \ \frac{\partial \sigma^+}{\partial t}(r, \varphi(r)) = \frac{\partial w^+}{\partial r}(r, \varphi(r)). \quad (45)$$

Let us introduce the notation

$$\sigma^*(r) \equiv \sigma(r, \varphi(r)), \quad (46)$$

differentiating which by the variable r we have:

$$\frac{d\sigma^*(r)}{dr} \equiv \frac{d\sigma(r, \varphi(r))}{dr} = \frac{\partial \sigma^+}{\partial t}(r, \varphi(r))\varphi'(r) + \frac{\partial \sigma^+}{\partial r}(r, \varphi(r)). \quad (47)$$

Substituting the relations (44)–(46) into (47) and expressing acceleration $a_\varphi(r)$ from the resulting formula, we have:

$$a_\varphi(r) = \frac{\frac{d\sigma^*(r)}{dr} + 2\frac{\sigma^*(r)}{r} - 3\alpha\kappa}{1 - \left(\varphi'(r)\right)^2}. \quad (48)$$

Now let us assume that a particle located at time t on the line $t = \varphi(r)$ has a positive velocity at the next moment of time. Then, it should be $a_\varphi(r) > 0$ at $\kappa = +1$. If this is not possible, then the second possible variant of motion with a negative velocity is analyzed, for which the inequality $a_\varphi(r) < 0$ must be fulfilled at $\kappa = -1$. If this also leads to a contradiction with Formula (48), then consequently $a_\varphi(r) = 0$, and a static equilibrium is established between the forces of elasticity and friction in the region $t > \varphi(r)$, described by the equation arising from (48):

$$\frac{d\sigma^*(r)}{dr} + 2\frac{\sigma^*(r)}{r} = 3\alpha\kappa(r). \quad (49)$$

Here $\sigma^*(r)$ is the residual distribution of tangential stresses after passing the stopping front $t = \varphi(r)$ (see the designation (46)). The frictional forces at the moment of stopping abruptly acquire values less than the maximum dry friction force, depending on the coordinate r and representing the $\kappa(r)$—part of its limiting value, so that the function $\kappa(r)$ is determined from Equation (49):

$$\kappa(r) = \frac{1}{3\alpha}\left(\frac{d\sigma^*(r)}{dr} + 2\frac{\sigma^*(r)}{r}\right), \quad |\kappa(r)| < 1. \tag{50}$$

Equating the expression (39) for velocity to zero, we obtain an implicit equation for determining the parametric family of zero velocity curves (by parameter α), i.e., the stopping (trailing) fronts of an elastic wave:

$$\frac{\alpha}{1+\alpha} = \frac{1}{r}\left(-2\frac{\mathrm{Re}\left[\bar{z}_0 \mathrm{K}_1(\bar{z}_0)\mathrm{K}_1(rz_0)\mathrm{e}^{z_0 t}\right]}{|z_0|^2|\mathrm{K}_1(z_0)|^2} - \int_0^\infty \frac{\mathrm{K}_1(rz)\mathrm{I}_2(z) + \mathrm{I}_1(rz)\mathrm{K}_2(z)}{\mathrm{K}_2^2(z) + \pi^2\mathrm{I}_2^2(z)}\frac{\mathrm{e}^{-tz}}{z}dz\right). \tag{51}$$

The zero velocity curves $t = \varphi(r;\alpha)$ are thus the level lines of the function on the right side of Equation (51).

Figure 3 shows curves $t = \varphi(r;\alpha)$, which are stopping (trailing) wave fronts, for the values of the parameter α equal 1/3, 1/7, 1/9, determined numerically based on Equation (51) using the Mathematica® application software package (version 13). As expected, the stopping fronts $t = \varphi(r;\alpha)$ of the plate sections at lower α (lower friction force) are located on the phase plane (r,t) above. Thus, the wave motion is carried out only in a bounded region of the phase plane (r,t), enclosed between the leading front of the wave $t = r - 1$ and the stopping front $t = \varphi(r;\alpha)$, whose position depends on the value of parameter α.

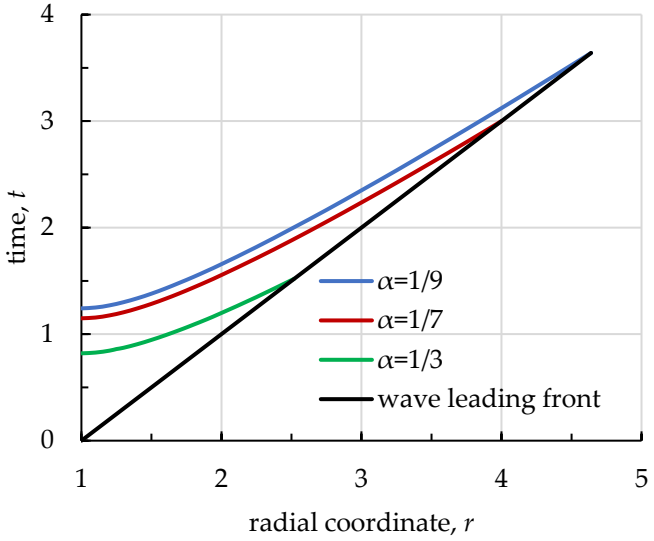

Figure 3. Elastic shear wave stopping fronts (trailing wave fronts) depending on the limiting value of the friction force (parameter α) in the phase plane (r,t).

4.3. Determination of Residual Stresses after Passing the Stop Front

Differentiating expressions (38) and (39) by time t gives under $t > r - 1$:

$$\frac{\partial\sigma}{\partial t}(r,t) = (1+\alpha)\left(2\frac{\mathrm{Re}\left[\mathrm{K}_1(\bar{z}_0)\mathrm{K}_2(rz_0)\mathrm{e}^{z_0 t}\right]}{|\mathrm{K}_1(z_0)|^2} + \int_0^\infty \frac{\mathrm{K}_2(rz)\mathrm{I}_2(z) - \mathrm{I}_2(rz)\mathrm{K}_2(z)}{\mathrm{K}_2^2(z) + \pi^2\mathrm{I}_2^2(z)}\mathrm{e}^{-tz}dz\right) \tag{52}$$

$$\frac{\partial w}{\partial t}(r,t) = -(1+\alpha)\left(2\frac{\mathrm{Re}\left[\mathrm{K}_1(\bar{z}_0)\mathrm{K}_1(rz_0)\mathrm{e}^{z_0 t}\right]}{\left|\mathrm{K}_1(z_0)\right|^2} - \int_0^\infty \frac{\mathrm{K}_1(rz)\mathrm{I}_2(z)+\mathrm{I}_1(rz)\mathrm{K}_2(z)}{\mathrm{K}_2^2(z)+\pi^2\mathrm{I}_2^2(z)}\mathrm{e}^{-tz}dz\right) \quad (53)$$

Further, since $\varphi'(r;\alpha) = -\frac{\partial\sigma}{\partial t}\Big|_{t=\varphi(r;\alpha)} \Big/ \frac{\partial w}{\partial t}\Big|_{t=\varphi(r;\alpha)}$, and $\frac{\partial\sigma}{\partial t}\Big|_{r=1,\,t=\varphi(1;\alpha)} = 0$ (see Equation (52)), then $\varphi'(1;\alpha) = 0$ for any values of α. Consequently, the initial velocity of propagation of the stopping front $t = \varphi(r;\alpha)$ is infinite. The analysis of the possibilities of motion in the region, carried out on the basis of the relation (48), shows that $t = \varphi(r;\alpha)$ is the trailing front of an elastic wave, so that after its passage a static equilibrium between elastic forces and friction forces is established on the plate sections $1 \le r \le r^*(\alpha)$, described by Equation (49). The distribution of residual stresses $\sigma^*(r)$ after passing the stopping front is shown in Figure 4 for three values of α.

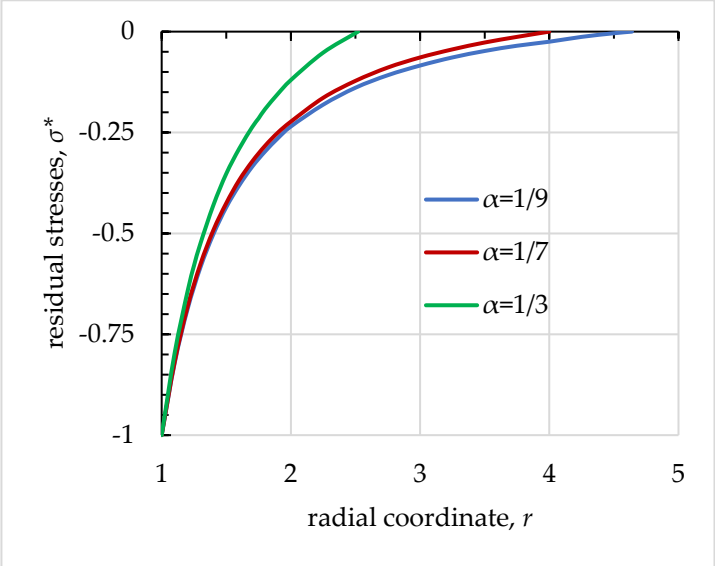

Figure 4. The distribution of residual stresses $\sigma^*(r)$ after the passage of the stopping front of the elastic shear wave, depending on the limiting friction force (parameter α).

It can be seen from Figure 4 that the larger the parameter α, the faster and on a shorter distance the residual tangential stresses $\sigma^*(r)$ decrease modulo from 1 to zero. In the cross section $r = r^*(\alpha)$, at the moment of time $t^*(\alpha) = r^*(\alpha) - 1$, a strong discontinuity degenerates at the leading front of the elastic wave $t = r - 1$, so that

$$\sigma^*(r^*) = 0,\ w(r^*, t^*) = 0 \quad (54)$$

and, therefore, $r^*(\alpha)$ is the maximum distance to which transverse elastic waves propagate in the plate. The value of r^*, as a function of the parameter α, is easy to determine by integrating the relations between the complete differentials of partial derivatives of the transversal displacement $u(r,t)$ ($v(r,t) = \frac{\partial u(r,t)}{\partial t}$) of the circular sections of the plate along the leading front $t = r - 1$. It can be shown, using system (1), that $u(r,t)$ satisfies the following hyperbolic differential equation:

$$\frac{\partial^2 u}{\partial r^2} + \frac{1}{r}\frac{\partial u}{\partial r} - \frac{u}{r^2} = \frac{\partial^2 u}{\partial t^2} + \mathrm{H}(t-r-1)q. \quad (55)$$

The characteristics of Equation (55) are straight lines $t = \pm r + C_{1,2}$ and along them, the characteristic conditions have the form:

$$du_r + \frac{1}{r}\left(u_r - \frac{u}{r}\right)dr = \pm du_t + qdr, \quad (56)$$

where specified $u_r \equiv \frac{\partial u}{\partial r}$, $u_t \equiv \frac{\partial u}{\partial t} = v$. Since on the leading front $t = r - 1$, the following relations are valid:

$$u|_{t=r-1} = 0,\ u_r|_{t=r-1} + u_t|_{t=r-1} = 0, \tag{57}$$

then, substituting them in (56), we obtain an ordinary differential equation for determining the velocity v on this front: $2dv + \frac{v}{r} = -qdr$. The solution of the last equation is $v = -\frac{A_0}{\sqrt{r}} - \frac{q}{3}r$, $(A_0 = const)$. Using the relation (57) and Hooke's law $\tau = u_r - \frac{u}{r}$, as well as the boundary condition (3), we find the velocity and stresses at the leading front:

$$v = \frac{\tau_0 + \frac{q}{3}}{\sqrt{r}} - \frac{q}{3}r,\ \tau = -\frac{\tau_0 + \frac{q}{3}}{\sqrt{r}} + \frac{q}{3}r \text{ at } t = r - 1. \tag{58}$$

Formula (58) with respect to the variables w and σ can be rewritten in the following form:

$$w = \frac{1+\alpha}{\sqrt{r}} - \alpha r,\ \sigma = -\frac{1+\alpha}{\sqrt{r}} + \alpha r \quad \text{at } t = r - 1. \tag{59}$$

From condition (54) we find a point on the phase plane where the shear wave is completely exhausted:

$$r^*(\alpha) = \sqrt[3]{\left(1 + \frac{1}{\alpha}\right)^2},\ t^*(\alpha) = \sqrt[3]{\left(1 + \frac{1}{\alpha}\right)^2} - 1. \tag{60}$$

4.4. Determination of Residual Stresses in the Case of Quasi-Static Loading

In the case of limiting equilibrium, when $\kappa = +1$, with quasi-static loading of the plate with the same load on the orifice boundary as in case of dynamic loading, the stress σ_{static} satisfies the equilibrium equation:

$$\frac{d\sigma_{\text{static}}}{dr} + 2\frac{\sigma_{\text{static}}}{r} = 3\alpha \tag{61}$$

and the condition at the boundary of the orifice $r = 1$ is

$$\sigma_{\text{static}} = -1. \tag{62}$$

The solution of the Cauchy problem (61) and (62) is easily obtained and the expression for σ_{static} has the form:

$$\sigma_{\text{static}} = -\frac{1+\alpha}{r^2} + \alpha r. \tag{63}$$

From (63) we find the boundary of the slip region in the case of realization of the limiting equilibrium:

$$r^*_{\text{static}}(\alpha) = \sqrt[3]{1 + \frac{1}{\alpha}}. \tag{64}$$

In the general case, when $0 < \kappa < 1$, the length of the slip area is obviously greater than in the limiting case (64):

$$r^*_{\text{static}}(\alpha) = \sqrt[3]{1 + \frac{1}{\kappa\alpha}}. \tag{65}$$

Comparing (60) and (64), we conclude that under dynamic loading, the length of the slip region (the region of motion) is significantly longer than under quasi-static (in the case of limiting equilibrium). In other words, there is a quadratic relationship between them: $r^*(\alpha) = \left(r^*_{\text{static}}(\alpha)\right)^2$.

It should be noted that the essential difference between the problem considered here and a similar problem for a semi-infinite rod (pipeline) immersed in an elastic Winkler medium with a friction force on its lateral surface depending on local deformation [7] is that during quasi-static loading of the rod, slippage between its lateral surface and the

environment occurs throughout the whole length of the rod. Here, for all possible states of static equilibrium, the area of slippage in the presence of friction is always finite (see Equation (65)).

4.5. Distribution of Friction Forces after Passing the Stopping Front

The nonlinear distribution of friction forces in the region $1 \le r \le r_*(\alpha)$ after passing the stopping front $t = \varphi(r;\alpha)$ becomes immediately known as soon as the function $\kappa = \kappa(r)$ is determined by Formula (50). Calculations show that $\kappa(r)$ does not always monotonically decrease from its maximum value at the boundary of the orifice $r = 1$ to the value in cross sections $r = r_*(\alpha)$. From Formula (50) and the equations of motion (40) and (41), one can obtain the expression:

$$\kappa(r) = 1 + \frac{1}{3\alpha a_\varphi(r)}\left(a_\varphi^2(r) - \left(\frac{\partial\sigma}{\partial t}(r;\varphi(r;\alpha))\right)^2\right) = 1 + \frac{a_\varphi(r)}{3\alpha}\left(1 - \left(\frac{d\varphi(r;\alpha)}{dr}\right)^2\right). \quad (66)$$

Acceleration graphs $a_\varphi(r)$ at the stopping front $t = \varphi(r;\alpha)$ of the plate sections, determined numerically using the Mathematica® application software package (version 13), are shown in Figure 5 for the values of the parameter α equal to $1/3$, $1/7$, $1/9$. From Formula (66), considering that $\frac{\partial\sigma}{\partial t}(1;t) = 0$, $\varphi'(1;\alpha) = 0$, it is possible to obtain values of $\kappa(r)$ on the motion region edges depending on the parameter α:

$$\kappa(1) = 1 + \frac{a_\varphi(1)}{3\alpha},\ \kappa(r^*) = -\frac{3\alpha}{4a_\varphi(r^*)}.$$

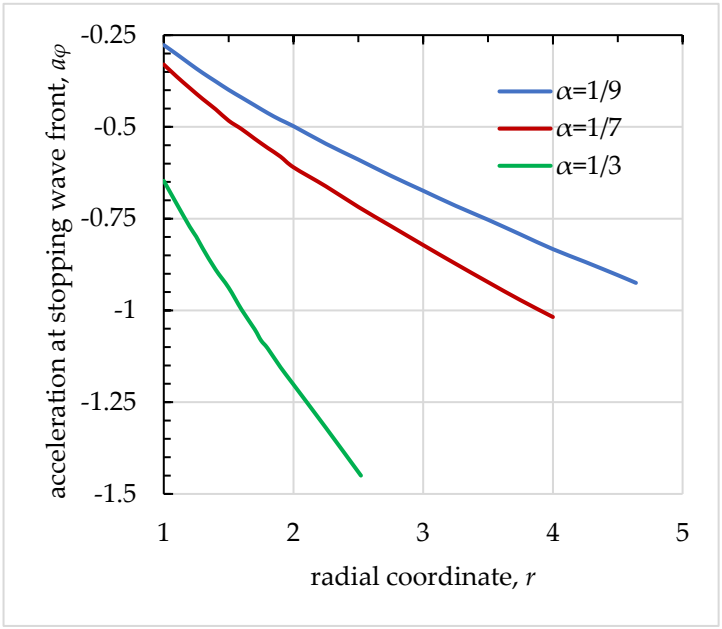

Figure 5. Distribution of accelerations $a_\varphi(r)$ at the stopping front of the elastic shear wave depending on the limiting friction force (parameter α).

Table 1 shows the values $r^*(\alpha)$—the distance at which the wave propagates, $t_*(\alpha) = \varphi(1;\alpha)$—the moment when the orifice boundary stops; the magnitudes of $\kappa(1)$ and $\kappa(r^*)$ for various α. Figure 6 shows the dependences of the residual friction force $\kappa(r)$ in various sections after passing the stopping front, depending on the magnitude of the limiting friction force α. It can be seen that the residual friction force does not always decrease monotonically from its value at the boundary of the orifice to the value in the elastic wave depletion section. The greatest drop in $\kappa(r)$ is observed near the boundary of the hole. At small relative values of the friction force ($\alpha = 1/9$), noticeable fluctuations of

the residual friction force are observed in the region of the plate through which the elastic shear wave passed.

Table 1. Stopping moments $t_*(\alpha)$ of the orifice boundary $r = 1$; maximum distances $r^*(\alpha)$ at which the elastic shear wave is depleted; distribution of residual friction forces $\kappa(1)$ and $\kappa(r^*)$ at the boundaries of the motion area.

α	$t_*(\alpha)$	$r^*(\alpha)$	$\kappa(1)$	$\kappa(r^*)$
1/3	0.82	2.52	0.35	0.17
1/7	1.15	4.00	0.23	0.11
1/9	1.24	4.64	0.17	0.09

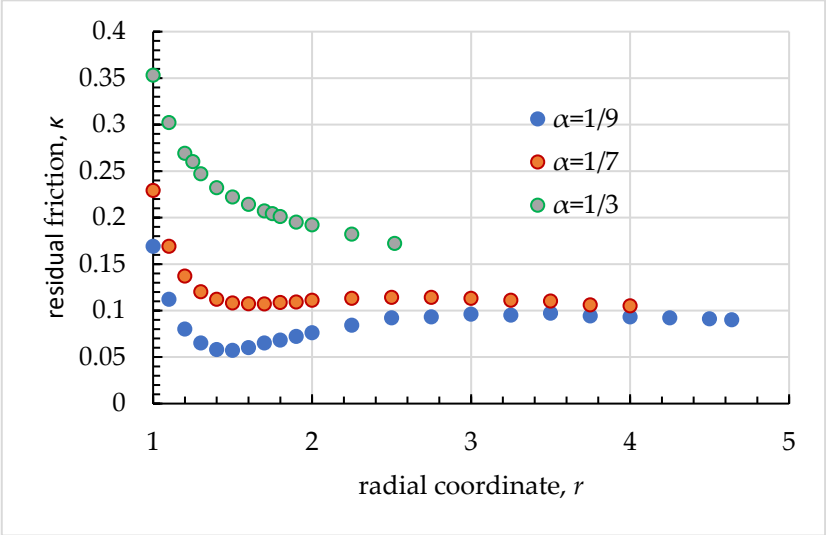

Figure 6. The distribution of the dimensionless residual friction force $\kappa(r)$ after passing the stopping front of the elastic shear wave as a function of the limiting friction force (parameter α).

5. Discussion

The results obtained in this study additionally allow us to establish new mathematical relations, as well as the solution of an important boundary value problem about a tangential impact on the surface of a cylindrical cavity in an elastic space.

Assuming $t = r - 1$ in Formulas (38) and (39) and comparing the obtained relations with the expressions (59) for σ and w on the leading front of the elastic shear wave, we have new identities valid for $r \geq 1$:

$$\int_0^\infty \frac{\mathrm{K}_2(rz)\mathrm{I}_2(z) - \mathrm{I}_2(rz)\mathrm{K}_2(z)}{\mathrm{K}_2^2(z) + \pi^2\mathrm{I}_2^2(z)} \frac{\mathrm{e}^{-(r-1)z}}{z} dz = \frac{1}{\sqrt{r}} - \frac{1}{r^2} + 2\frac{\mathrm{Re}\left[\bar{z}_0\mathrm{K}_1(\bar{z}_0)\mathrm{K}_2(rz_0)\mathrm{e}^{z_0(r-1)}\right]}{|z_0|^2|\mathrm{K}_1(z_0)|^2}, \tag{67}$$

$$\int_0^\infty \frac{\mathrm{K}_1(rz)\mathrm{I}_2(z) + \mathrm{I}_1(rz)\mathrm{K}_2(z)}{\mathrm{K}_2^2(z) + \pi^2\mathrm{I}_2^2(z)} \frac{\mathrm{e}^{-(r-1)z}}{z} dz = -\frac{1}{\sqrt{r}} - 2\frac{\mathrm{Re}\left[\bar{z}_0\mathrm{K}_1(\bar{z}_0)\mathrm{K}_1(rz_0)\mathrm{e}^{z_0(r-1)}\right]}{|z_0|^2|\mathrm{K}_1(z_0)|^2}, \tag{68}$$

which are not found, apparently, in the well-known literature. Substitute $r = 1$ into Formula (68), then considering the identity $\mathrm{K}_1(z)\mathrm{I}_2(z) + \mathrm{K}_2(z)\mathrm{I}_1(z) = 1/z$ known in the theory of Bessel functions [8], it will be written in the following form (see (19)):

$$\int_0^\infty \frac{1}{\mathrm{K}_2^2(z) + \pi^2\mathrm{I}_2^2(z)} \frac{1}{z^2} dz = -1 - 2\frac{\mathrm{Re}[\bar{z}_0]}{|z_0|^2} = -1 + \frac{2x_0}{x_0^2 + y_0^2} \approx 0.4031872.$$

Checking the resulting integral with the help of the NIntegrate utility of the Mathematica® computing shell (version 13) naturally gives the same result.

If we put $\alpha = 0$ in expressions (39) and (40), then as a result, we immediately have an exact solution to the axisymmetric problem of the propagation of shear elastic waves in an infinite isotropic space with a cylindrical cavity $r = 1$, when the shock tangent stresses $\sigma(1,t) = -\mathrm{H}(t)$ are set on its boundary (plane problem):

$$\sigma(r,t) = \left(-\frac{1}{r^2} + 2\frac{\mathrm{Re}\left[\bar{z}_0 \mathrm{K}_1(\bar{z}_0)\mathrm{K}_2(rz_0)\mathrm{e}^{z_0 t}\right]}{|z_0|^2 |\mathrm{K}_1(z_0)|^2} - \int_0^\infty \frac{\mathrm{K}_2(rz)\mathrm{I}_2(z) - \mathrm{I}_2(rz)\mathrm{K}_2(z)}{\mathrm{K}_2^2(z) + \pi^2 \mathrm{I}_2^2(z)} \frac{\mathrm{e}^{-tz}}{z} dz \right) \mathrm{H}(t - r + 1), \tag{69}$$

$$w(r,t) = \left(-2\frac{\mathrm{Re}\left[\bar{z}_0 \mathrm{K}_1(\bar{z}_0)\mathrm{K}_1(rz_0)\mathrm{e}^{z_0 t}\right]}{|z_0|^2 |\mathrm{K}_1(z_0)|^2} - \int_0^\infty \frac{\mathrm{K}_1(rz)\mathrm{I}_2(z) + \mathrm{I}_1(rz)\mathrm{K}_2(z)}{\mathrm{K}_2^2(z) + \pi^2 \mathrm{I}_2^2(z)} \frac{\mathrm{e}^{-tz}}{z} dz \right) \mathrm{H}(t - r + 1). \tag{70}$$

From Formula (70) it is easy to obtain the law of change of the transversal velocity in time on the boundary of the cylindrical cavity:

$$w(1,t) = 2\frac{x_0 \cos(y_0 t) - y_0 \sin(y_0 t)}{x_0^2 + y_0^2} \mathrm{e}^{-x_0 t} - \int_0^\infty \frac{1}{\mathrm{K}_2^2(z) + \pi^2 \mathrm{I}_2^2(z)} \frac{\mathrm{e}^{-tz}}{z^2} dz,$$

so at the moment of time $t = 0$, the boundary abruptly acquires velocity $w(1,0) = 1$. When $t \to \infty$, both terms in the last formula tend to zero; that is, the shear wave exponentially decays in time.

In conclusion, we note that Formula (6) indicates a method for determining the magnitude of the limiting friction force. Indeed, by measuring the velocity jump w_1 in any circular section $r = r_1$ of the plate at the time of the passage of the leading front $t = r - 1$, we easily find the value of α by Formula (59), $\alpha = \frac{1 - w_1\sqrt{r_1}}{\sqrt{r_1^3 - 1}}$, and consequently the depletion coordinate $r^*(\alpha)$ (see Equation (60)) of the leading front of the shear wave.

6. Conclusions

An exact analytical solution of the problem of the propagation of elastic shear waves in a plate interacting with a rigid rough base according to Coulomb's dry friction law in the case of a tangential impact on the surface of a circular hole is obtained. Depending on the ratio of the specific friction force to the load amplitude, the finite areas of motion in the plate and the radius of complete exhaustion of the wave front are determined. In the future, it is projected to consider similar boundary value problems with a different type of load on the boundary of the hole in the plate.

Awkwardly, there are no articles in known literature where dynamic problems for plates on a rough base are considered. In the introduction, we analyzed the few articles considering wave propagation in rods with external friction that are directly or indirectly related to the subject of research in our work. In [4], for example, the propagation of a longitudinal but not shear wave in a cylindrical semi-infinite rod surrounded by a rigid medium is considered, accounting for the dry friction occurring at the interface and depending on deformation of the cross sections of the rod. A shock load is instantly applied to the butt of the rod and maintained constant over time. The problem is solved in a one-dimensional formulation and an analytical solution has been found at the front of the strong rupture wave for stresses that decrease exponentially with distance from the end section of the rod. In fact, this solution to a similar problem was first found earlier in my work [7], and not only at the wave front, but also in the area beyond this front, up to the stopping front.

Along the way, for the first time, a precise analytical solution was obtained to the boundary value problem of the propagation of elastic shear waves in an infinite isotropic space with a cylindrical cavity, when a tangential shock load is set on its surface.

Funding: This research received no external funding.

Data Availability Statement: Data sharing is not applicable. The article describes entirely theoretical research.

Conflicts of Interest: The author declares no conflict of interest.

References

1. Mogilevsky, R.I.; Ormonbekov, T.O.; Nikitin, L.V. Dynamics of Rods with Interfacial Dry Friction. *J. Mech. Behav. Mater.* **1993**, *5*, 85–93. [CrossRef]
2. Nikitin, L.V. *Statics and Dynamics of Solids with External Dry Friction*; Moskovskyi Litsei: Moscow, Russia, 1998. (In Russian)
3. Kharchenko, Y.; Hutyi, A.; Haiduk, V. The Influence of Friction Forces on Longitudinal Wave Propagation in a Stuck Drill String in a Borehole. *Tribologia* **2018**, *6*, 79–87. [CrossRef]
4. Sultanov, K.S.; Khusanov, B.E.; Rikhsieva, B.B. Elastic wave propagation in a cylinder with external active friction. *J. Phys. Conf. Ser.* **2021**, *1901*, 012125. [CrossRef]
5. Karachevtseva, I.; Dyskin, A.V.; Pasternak, E. Generation and propagation of stick-slip waves over a fault with rate-independent friction. *Nonlin. Process. Geophys.* **2017**, *24*, 343–349. [CrossRef]
6. Shatskyi, I.; Perepichka, V.; Vaskovskyi, M. Longitudinal waves in an Elastic Rod Caused by Sudden Damage to the Foundation. *Theor. Appl. Mech.* **2021**, *48*, 29–37. [CrossRef]
7. Filippov, A.N. Dynamic Impact on a Pipeline Considering Dry Friction on its Surface. *Mech. Solids* **2019**, *54*, 1144–1150. [CrossRef]
8. Watson, G.N. *A Treatise on the Theory of Bessel Functions*, 2nd ed.; The Macmillan Company: New York, NY, USA, 1944.
9. Kerimov, M.K.; Skorokhodov, S.L. Calculation of the Complex Zeros of the Modified Bessel Function of the Second Kind and its Derivatives. *U.S.S.R. Comput. Math. Math. Phys.* **1984**, *24*, 115–123. [CrossRef]
10. Markushevich, A.M. *The Theory of Analytic Functions: A Short Course*; MIR Publishers: Moscow, Russia, 1983.
11. Ditkin, V.A.; Prudnikov, A.P. *Handbook of Operational Calculus*; Vysshaya shkola: Moscow, Russia, 1965. (In Russian)